

Mononuclear Fe(III) Complex Showing Thermally Induced Spin Crossover and Slow Magnetic Relaxation with Reciprocating Thermal Behaviour

Terézia Bridová, Cyril Rajnák, Ján Titiš, Erika Samoľová, Kevin Tran, Ondrej Malina, Alina Bieńko Franz Renz, Milan Gembický and Roman Boča

Supplementary Information

Elemental analysis was carried out by Flash 2000 CHNS apparatus (Thermo Scientific).

Absorption spectra in the UV–Vis region (9000 – 50 000 cm⁻¹) were recorded by UV–Vis–NIR spectrophotometer (Varian, 50 Bio).

FT-IR spectra were measured by ATR method in region 400 – 4000 cm⁻¹ at room temperature (Shimadzu IRAffinity-1, Quest ATR holder). Absorption spectra in the UV–Vis region (9000 – 50 000 cm⁻¹) were recorded by UV–Vis–NIR spectrophotometer (Varian, 50 Bio).

Single-crystal X-ray diffraction data studies were carried out on Bruker APEX-II CCD equipped with a CCD Area Detector and MoK α radiation ($\lambda = 0.7107 \text{ \AA}$) Data were collected using ϕ and ω scans in a nitrogen gas stream at 100 and 293 K. The data were integrated using the Bruker SAINT Software program and scaled using the SADABS software program.^{S1} The structure was solved with the ShelXT solution program using direct methods. The model was refined with XL using full-matrix least-squares minimization on F2 using Olex2 1.5 as the graphical interface.^{S2,S3} All nonhydrogen atoms were refined anisotropically by full-matrix least-squares (SHELXL-2014). All carbon bonded hydrogen atoms were placed using a riding model. Their positions were constrained relative to their parent atom using the appropriate HFIX command in SHELXL-2014. The disordered EtO parts were refined using a SADI and EADP commands. Molecular graphics were created by Diamond 4 program.^{S4}

Ab initio calculations were done at the CASSCF level followed by NEVPT2 module have been conducted using the ORCA package.^{S5-S7} The active space consists of 5 electrons distributed in 5 d-orbitals giving rise to 75 doublets, 24 quartets and 1 sextet states, in total 252 states. Experimental geometries of complexes were used and ZORA-def2-TZVPP for the Fe atom and ZORA-def2-SV(P) for the remaining atoms formed the basis set yielding 622 basis functions. The spin-orbit coupling has been treated using the SOMF approximation.

Mössbauer spectroscopy was performed with a customized WISSEL drive setup in transmission mode using a MIMOS II silicon pin detector. Co-57 in a Rh matrix was used as the Mössbauer source. The sample was cooled with liquid nitrogen to 77 K und measured for 3 days. The calibration and fitting were done with the data processing tool “Recoil” with the least squares method. All values are in relation to α -Fe.

The magnetic data was acquired with the help of the SQUID magnetometer (MPMS3, Quantum Design) at the vsm data taking modes. DC magnetic susceptibility was taken at $B_{DC} = 0.1 \text{ T}$ between 2 and 400 K; magnetization at $T = 2.0$ and 4.6 K until $B_{DC} = 9.0 \text{ T}$. AC susceptibility measurements were conducted with the MPMS apparatus using amplitude $B_{AC} = 0.3 \text{ mT}$ and five scans. SI units are employed.

The fitting procedure has been assessed by two criteria: the discrepancy factor for in-phase and out-of-phase susceptibility, $R(\chi')$ and $R(\chi'')$, respectively, and the standard deviation of each optimized parameter (see SI).

[S1] Sadabs: Bruker (2001). SADABS. Bruker AXS Inc., Madison, Wisconsin, USA.

[S2] O. V. Dolomanov, L. J. Bourhis, R. J. Gildea, J. A. K. Howard, H. Puschmann, OLEX2: a complete structure solution, refinement and analysis program, *J. Appl. Cryst.*, 2009, **42**, 339-341.

[S3] G. M. Sheldrick, SHELXT – Integrated space-group and crystal structure determination, *Acta Cryst.*, 2015, **A71**, 3.

[S4] Diamond: Brandenburg, K. (1999). DIAMOND. Version 4.6.4. Crystal Impact GbR, Bonn, Germany.

[S5] F. Neese, The ORCA program system, *WIREs Comput Mol Sci.*, 2012, **2**, 73-78.

[S6] F. Neese, ORCA - An Ab Initio, Density Functional and Semi-empirical Program Package, version 5.0.2; 2022.

Mononuclear Fe(III) Complex Showing Thermally Induced Spin Crossover and Slow Magnetic Relaxation with Reciprocating Thermal Behaviour

Terézia Bridová, Cyril Rajnák, Ján Titiš, Erika Samoľová, Kevin Tran, Ondrej Malina, Alina Bieňko, Franz Renz, Milan Gembický and Roman Boča

[S7] F. Neese, F. Wennmohs, U. Becker, C. Riplinger, The ORCA quantum chemistry program package, *J. Chem. Phys.*, 2020, **152**, 224108.

Synthesis of [Fe(L⁵)(Cl)] type precursor

N-(2-aminoethyl)-1,3-propanediamine (2 mmol) and 3-ethoxysalicylaldehyde (4 mmol) were dissolved in 10 cm³ of methanol. The solution was stirred and heated under reflux for 30 min, FeCl₃·6H₂O (4 mmol) in 20 cm³ methanol was added and further stirred and heated under reflux for 1 h. Finally, the solution was kept at -15°C in a fridge for a few days, the black microcrystalline product was filtered over the ashless paper and fritted glass and dried at room temperature. *Anal. Calc.* for C₂₄H₂₉FeN₄O₄Se (572.32 g·mol⁻¹): Teo.: C, 50.37; H, 5.11; N, 9.79. Exp.: C, 50.14; H, 5.06; N, 9.76. Selected IR bands (ATR) ν/cm⁻¹: 13177; 2972; 2911; 2849; 2095; 2057; 1608; 1539; 1417; 1394; 1303; 1242; 1212; 1074; 1051; 998; 884; 838; 732; 625; 571; 435. UV/Vis (Acetonitrile) ν_{max}/10³ cm⁻¹ (relat. absorb.): 18.20 (0.05); 28.87 (0.19); 37.43 (0.57); 43.85 (1.08).

Synthesis of complex [Fe(L⁵)(NCSe)]

The complex [Fe(L⁵)(Cl)] (0.36 mmol) was dissolved in 20 cm³ methanol stirred for 15 min. Afterwards a solution of pseudohalide salt KNCS_e (0.36 mmol) in 10 cm³ methanol was added. The mixture was stirred and heated under reflux for 3 h. After 3 h the mixture was put into an ultrasonic bath for 20 min. and filtered with a paper filter. Dark violet crystals were isolated after few days by the filtration from mother liquid. *Anal. Calc.* for C₂₄H₂₉FeN₄O₄Se (572.32 g·mol⁻¹): Teo.: C, 50.37; H, 5.11; N, 9.79. Exp.: C, 50.14; H, 5.06; N, 9.76. Selected IR bands (ATR) ν/cm⁻¹: 13177; 2972; 2911; 2849; 2095; 2057; 1608; 1539; 1417; 1394; 1303; 1242; 1212; 1074; 1051; 998; 884; 838; 732; 625; 571; 435. UV/Vis (Acetonitrile) ν_{max}/10³ cm⁻¹ (relat. absorb.): 18.20 (0.05); 28.87 (0.19); 37.43 (0.57); 43.85 (1.08).

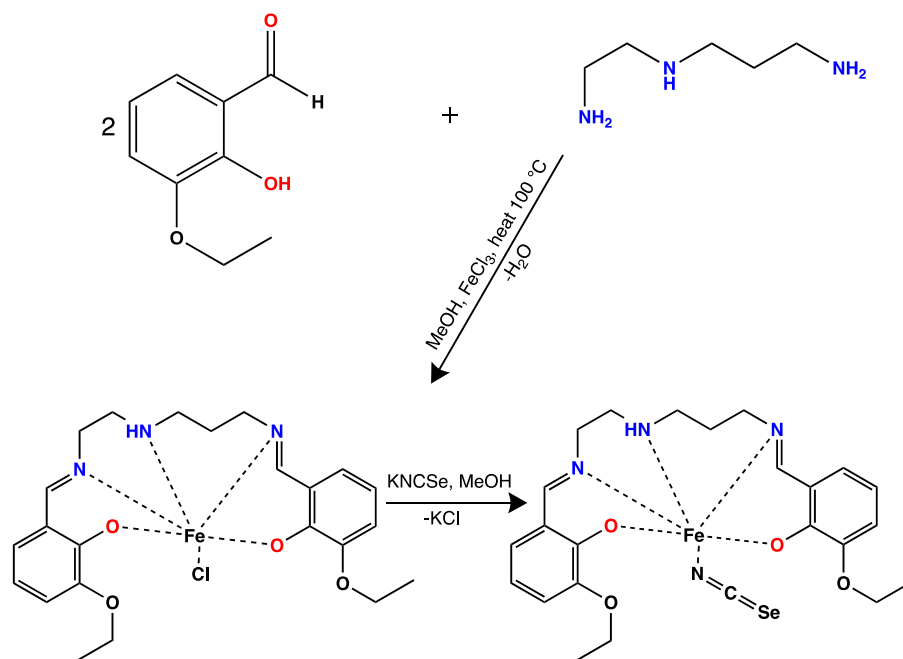


Figure S1. Synthesis of complex [Fe(L⁵)(NCSe)].

Mononuclear Fe(III) Complex Showing Thermally Induced Spin Crossover and Slow Magnetic Relaxation with Reciprocating Thermal Behaviour

Terézia Bridová, Cyril Rajnák, Ján Titiš, Erika Samoľová, Kevin Tran, Ondrej Malina, Alina Bieňko, Franz Renz, Milan Gembický and Roman Boča

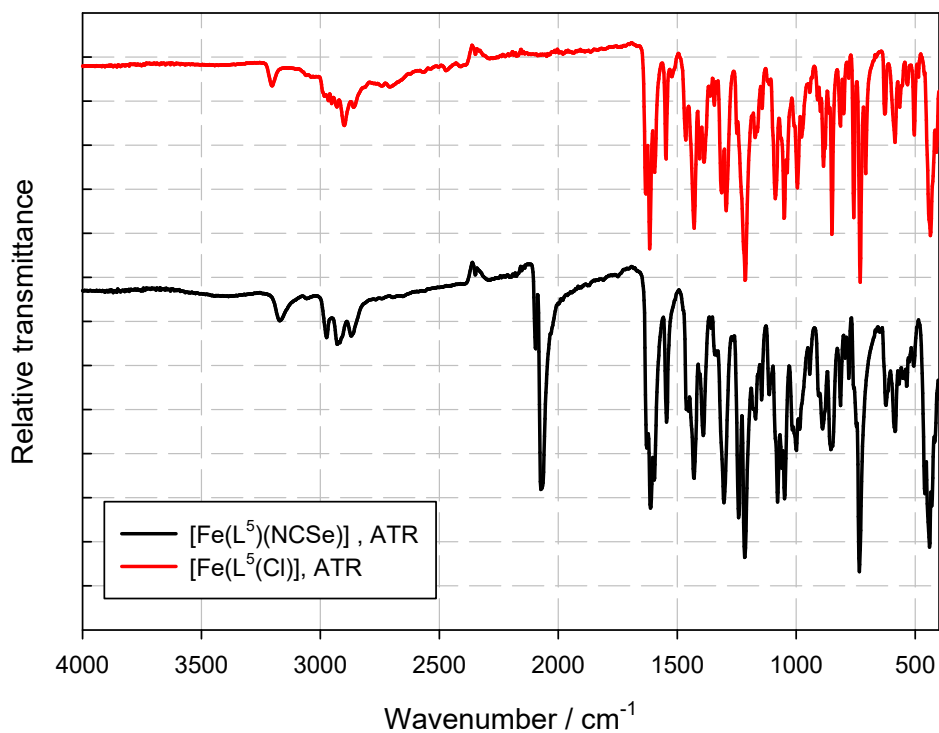


Figure S2. FT-IR spectrum of complex **1** and its precursor.



Figure S3. A reversible thermochromism from black $T = 297$ K to dark-green at $T = 77$ K (cooled with the liquid nitrogen).

Mononuclear Fe(III) Complex Showing Thermally Induced Spin Crossover and Slow Magnetic Relaxation with Reciprocating Thermal Behaviour

Terézia Bridová, Cyril Rajnák, Ján Titiš, Erika Samoľová, Kevin Tran, Ondrej Malina, Alina Bieňko, Franz Renz, Milan Gembický and Roman Boča

Table S1. Crystal data and structure refinement parameters of **1a** and **1b**.

	1a , [Fe ^{III} (L ⁵)NCSe]	1b , [Fe ^{III} (L ⁵)NCSe]
Empirical formula	C ₂₄ H ₂₉ FeN ₄ O ₄ Se _{0.96}	C ₂₄ H ₂₉ FeN ₄ O ₄ Se
Formula weight	569.16	572.32
Temperature/K	293	100
Crystal system	monoclinic	monoclinic
Space group	<i>P2₁/n</i>	<i>P2₁/n</i>
<i>a</i> /Å	15.4057(17)	14.8710(4)
<i>b</i> /Å	13.593(2)	13.4451(4)
<i>c</i> /Å	24.030(3)	24.1768(9)
α /°	90	90
β /°	93.079(4)	93.522(1)
γ /°	90	90
Volume/Å ³	5024.8 (12)	4824.8(3)
<i>Z</i>	8	8
ρ_{calc} g/cm ³	1.505	1.576
μ /mm ⁻¹	2.03	2.17
<i>F</i> (000)	2333	2344
Crystal size/mm ³	0.18 × 0.17 × 0.12	0.18 × 0.17 × 0.12
Radiation	Mo K α (λ = 0.71073)	Mo K α (λ = 0.71073)
2 Θ range /°	1.534 to 25.726	2.707 to 27.139
Index ranges	-18 ≤ <i>h</i> ≤ 18, -16 ≤ <i>k</i> ≤ 16, -29 ≤ <i>l</i> ≤ 29	-19 ≤ <i>h</i> ≤ 18, -17 ≤ <i>k</i> ≤ 17, -31 ≤ <i>l</i> ≤ 31
Reflections collected	136965	118160
Independent reflections	9548 [<i>R</i> _{int} = 0.067, <i>R</i> _{sigma} = 0.0611]	10648 [<i>R</i> _{int} = 0.041, <i>R</i> _{sigma} = 0.030]
Data/restraints/parameters	9548/66/675	10648/12/645
Goodness-of-fit on <i>F</i> ²	1.019	1.026
Final <i>R</i> indexes [<i>I</i> >= 2 σ (<i>I</i>)]	<i>R</i> ₁ = 0.0359, <i>wR</i> ₂ = 0.0794	<i>R</i> ₁ = 0.0254, <i>wR</i> ₂ = 0.0693
Final <i>R</i> indexes [all data]	<i>R</i> ₁ = 0.0611, <i>wR</i> ₂ = 0.0903	<i>R</i> ₁ = 0.0300, <i>wR</i> ₂ = 0.0725
Largest diff. peak/hole / e Å ⁻³	0.482/-0.595	0.875/-0.832
Color	black	metallic black
CCDC No	2252251	2252250

Mononuclear Fe(III) Complex Showing Thermally Induced Spin Crossover and Slow Magnetic Relaxation with Reciprocating Thermal Behaviour

Terézia Bridová, Cyril Rajnák, Ján Titiš, Erika Samoľová, Kevin Tran, Ondrej Malina, Alina Bieňko, Franz Renz, Milan Gembický and Roman Boča

Note: communication between referee and authors

<p>Crystallographer: Comments to the Author Please see attached files. There are 2 structures in this paper. We examined CCDC 2252250-2252251</p> <p>Thanks to the author for the comments. Unfortunately, I cannot agree with them because they ignore the following aspects:</p> <p>“We are aware that the Se1 atom appears less than 100% occupied, but since this is only the case for one of the two chemically identical molecules in this structure, we decided to keep the occupancy at 1 for both Se.”</p> <p>There are two molecules per asymmetric unit. Although they may be chemically identical, they do not appear identical in the crystal. This is very strange and needs an explanation, but it can not be ignored. My previous suggestion with the Se/S disorder is the simplest explanation that comes to mind -- although why the disorder would only happen in *one* of the molecules is a mystery.</p> <p>“The resulting difference Fourier map does show a negative maximum around the Se1 atom, but the size of it doesn't lead to alerts A and B during the Checkcif procedure.”</p> <p>This is typical for atom positions that are not 100% occupied. And just because Checkcif doesn't generate an alert A or B, a structure doesn't have to be correct. As you can see from the attached images, this is not a minor effect, but a serious issue. 10% of a Se is a large discrepancy.</p> <p>“None of performed chemical analyses supported the presence of the disorder in this position. If the NCSe particle were decomposing, and the NCSe/CN disorder was present, we would expect the presence of specific vibrational bands of the CN group in the IR spectrum. This was not confirmed. Elemental analysis also</p>	<p>Response:</p> <p>Dear crystallographer,</p> <p>To elucidate the “depletion” of the electron density on one of the Se atom positions on the selenocyanate group we have made additional diffraction experiments.</p> <p>3 Crystals have been measured, with a total of 5 complete measurements, two at Room Temperature and three 100K data collection.</p> <p>Refinement using these new experimental data was consistent with previous observation and a similar electron density deficit was observed on one of the Selenium atom positions.</p> <p>A freely refined Se atom position would indicate approximately 95 % occupancy, or 5 % deficit.</p> <p>Note the asymmetric unit contains two FeL5CNSe molecules, assuming this would be impurity in the sample, the molar ratio would be approximately 2.5 %</p> <p>Only explanation would be that the starting KSeCN contains minor cyanide impurities such as they co-crystallize with preferential (possibly due to minor differences in the packing environment).</p>
---	--

Mononuclear Fe(III) Complex Showing Thermally Induced Spin Crossover and Slow Magnetic Relaxation with Reciprocating Thermal Behaviour

Terézia Bridová, Cyril Rajnák, Ján Titiš, Erika Samoľová, Kevin Tran, Ondrej Malina, Alina Bieńko, Franz Renz, Milan Gembický and Roman Boča

showed excellent agreement with the expected composition, as shown in Supplementary Information file.”

All of these methods are studies on bulk material. SC-XRD examines a single crystal and can provide different results. Crystallisation is a very powerful separation method.

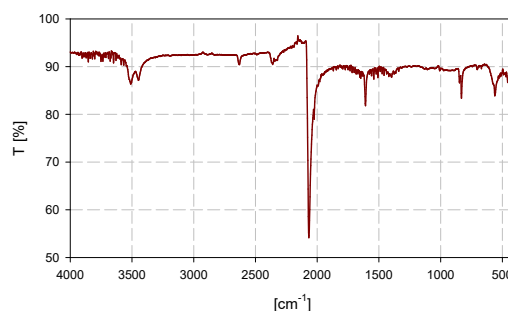
“Moreover, no sulfur-containing compound was used during the synthesis. The reaction of precursor Fe(L)Cl with KNCS_e runs in methanol. Therefore, Se/S disorder can not be present.”

I don't know what purity the starting substances were, but experience has shown that selenium compounds are almost always contaminated with sulfur.

Therefore, I cannot recommend publishing these structures if the negative electron density at one selenium position is ignored.

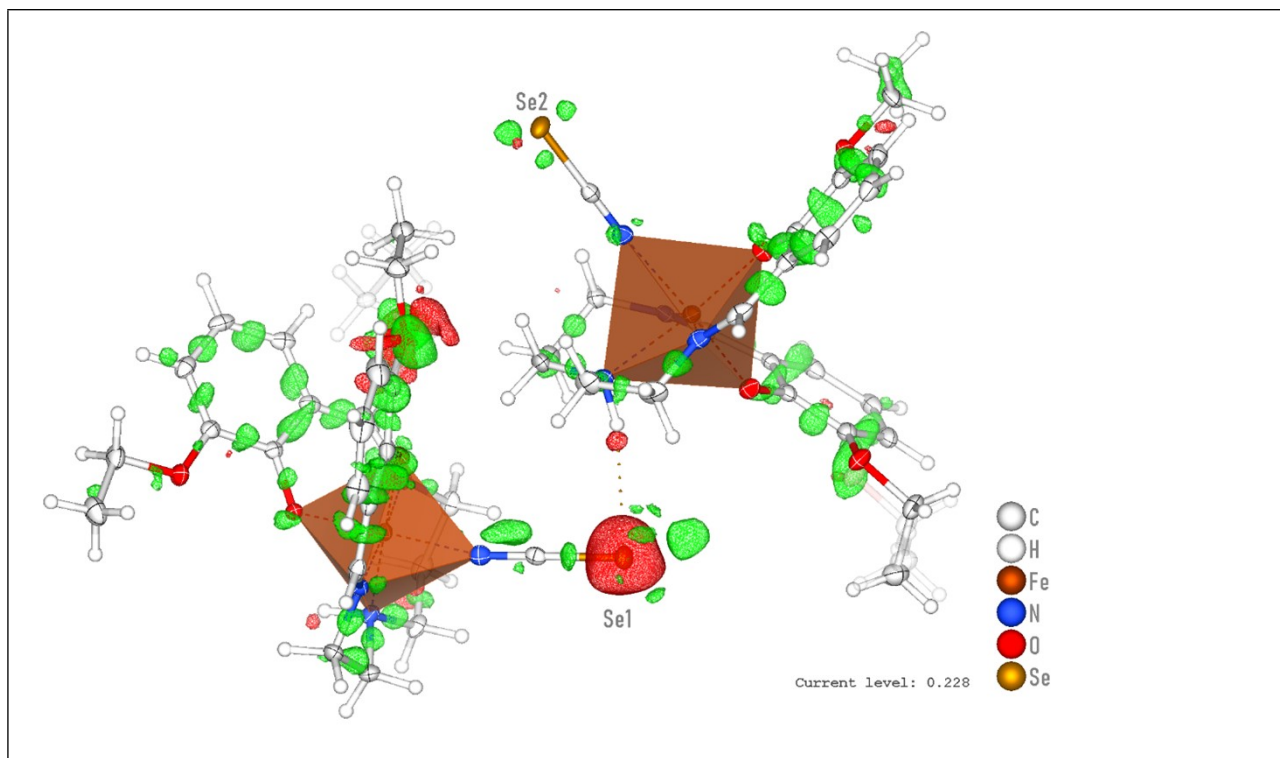
Thank you.

We measured FTIR-ATR of pure reagent ($\geq 99\%$). Our device (Shimadzu IRAffinity-1, Quest ATR holder) is not able to detect potential minor CN contamination.

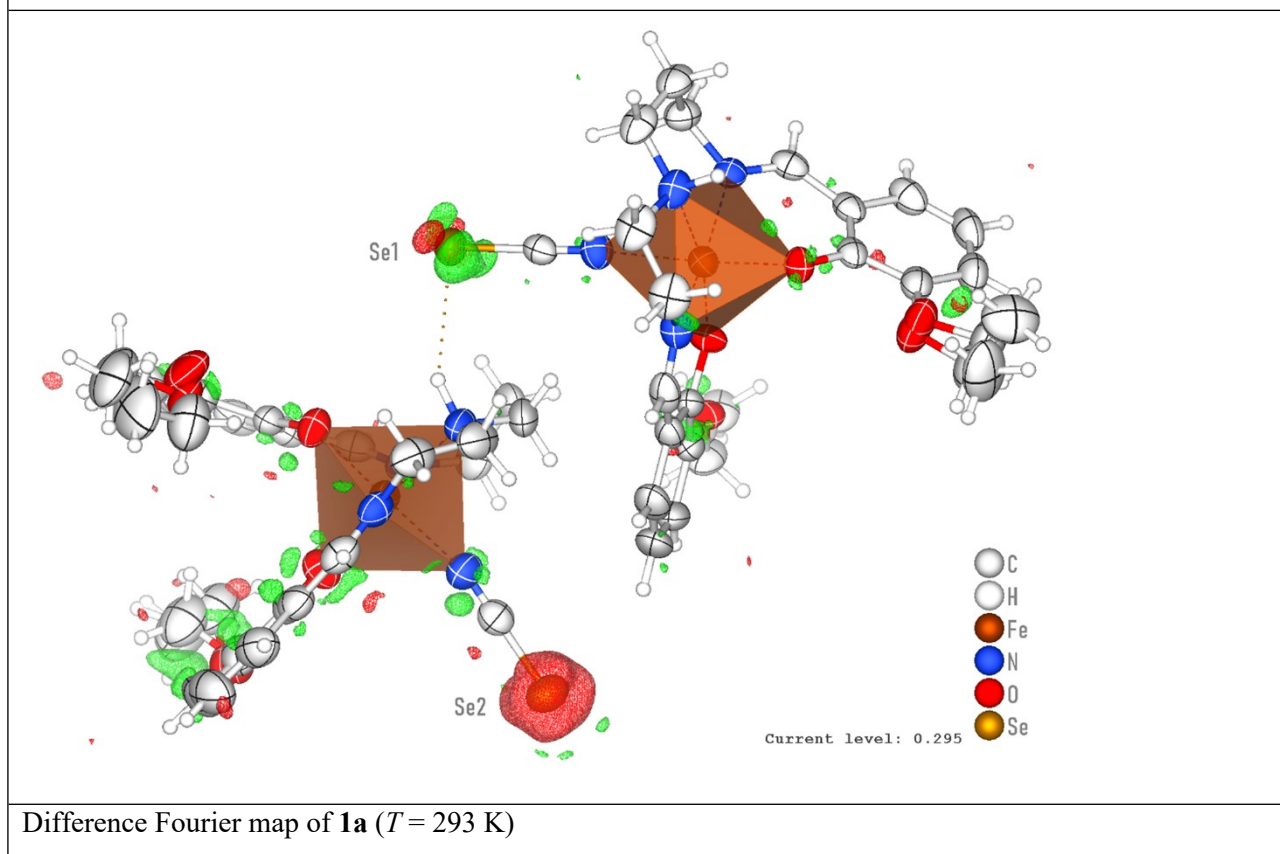


Mononuclear Fe(III) Complex Showing Thermally Induced Spin Crossover and Slow Magnetic Relaxation with Reciprocating Thermal Behaviour

Terézia Bridová, Cyril Rajnák, Ján Titiš, Erika Samoľová, Kevin Tran, Ondrej Malina, Alina Bieňko, Franz Renz, Milan Gembický and Roman Boča



Difference Fourier map of **1b** ($T = 100$ K)



Difference Fourier map of **1a** ($T = 293$ K)

Mononuclear Fe(III) Complex Showing Thermally Induced Spin Crossover and Slow Magnetic Relaxation with Reciprocating Thermal Behaviour

Terézia Bridová, Cyril Rajnák, Ján Titiš, Erika Samoľová, Kevin Tran, Ondrej Malina, Alina Bieňko, Franz Renz, Milan Gembický and Roman Boča

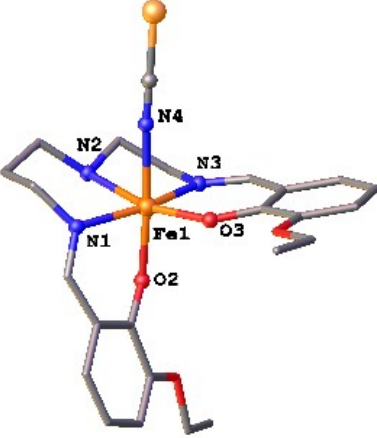
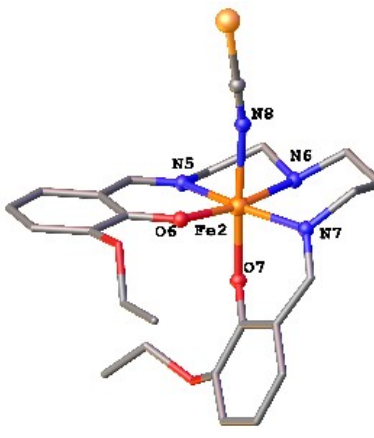
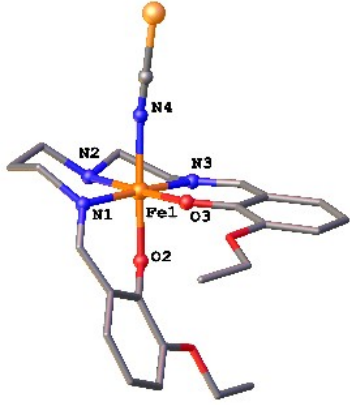
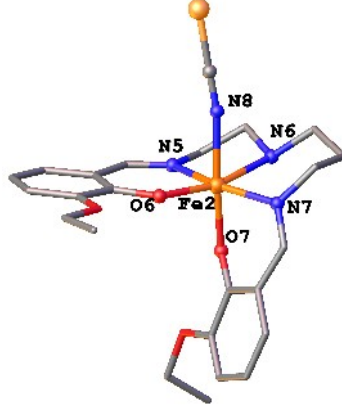
1a, unit_A		1a, unit_B	
			
N1-Fe1	2.088(2)	N5-Fe2	2.043(3)
N2-Fe1	2.225(2)	N6-Fe2	2.132(3)
N3-Fe1	2.084(2)	N7-Fe2	2.048(3)
N4-Fe1	2.160(3)	N8-Fe2	2.128(3)
O2-Fe1	1.9472(18)	O6-Fe2	1.885(2)
O3-Fe1	1.9115(18)	O7-Fe2	1.9192(19)
1b, unit_A		1b, unit_B	
			
N1-Fe1	1.9582(15)	N5-Fe2	2.0966(15)
N2-Fe1	2.0059(15)	N6-Fe2	2.2109(15)
N3-Fe1	1.9228(15)	N7-Fe2	2.0923(15)
N4-Fe1	1.9859(16)	N8-Fe2	2.1555(15)
O2-Fe1	1.8673(12)	O6-Fe2	1.9179(13)
O3-Fe1	1.8677(13)	O7-Fe2	1.9482(13)

Figure S4. Molecular structure of **1a** at $T = 293$ K and **1b** at $T = 100$ K. Colour code: blue-nitrogen, red-oxygen, orange-iron, grey-carbon, yellow-selenium. Hydrogen atoms are omitted for clarity. Metal-ligand distance in Å.

Mononuclear Fe(III) Complex Showing Thermally Induced Spin Crossover and Slow Magnetic Relaxation with Reciprocating Thermal Behaviour

Terézia Bridová, Cyril Rajnák, Ján Titiš, Erika Samoľová, Kevin Tran, Ondrej Malina, Alina Bieňko, Franz Renz, Milan Gembický and Roman Boča

Table S2. Selected bond angles (deg) in chromophores {FeN₄O₂} of complex **1**.

1a Unit A		1a Unit B		1b Unit A		1b Unit B	
O2-Fe1-O3	95.57(8)	O6-Fe2-O7	93.64(9)	O2-Fe1-O3	91.42(6)	O6-Fe2-O7	95.42(6)
O2-Fe1-N1	85.40(8)	O6-Fe2-N5	90.52(10)	O2-Fe1-N1	90.11(6)	O6-Fe2-N5	88.82(6)
O2-Fe1-N2	93.45(8)	O6-Fe2-N6	169.84(10)	O2-Fe1-N2	89.97(6)	O6-Fe2-N6	164.99(6)
O2-Fe1-N3	90.83(8)	O6-Fe2-N7	100.84(10)	O2-Fe1-N3	86.57(6)	O6-Fe2-N7	108.24(5)
O2-Fe1-N4	175.99(9)	O6-Fe2-N8	87.56(10)	O2-Fe1-N4	178.14(6)	O6-Fe2-N8	88.01(6)
O3-Fe1-N1	109.01(8)	O7-Fe2-N5	90.55(9)	O3-Fe1-N1	88.29(6)	O7-Fe2-N5	89.67(6)
O3-Fe1-N2	164.52(8)	O7-Fe2-N6	91.79(9)	O3-Fe1-N2	178.61(6)	O7-Fe2-N6	93.21(6)
O3-Fe1-N3	89.01(9)	O7-Fe2-N7	86.48(9)	O3-Fe1-N3	95.10(6)	O7-Fe2-N7	86.03(6)
O3-Fe1-N4	87.69(9)	O7-Fe2-N8	177.26(10)	O3-Fe1-N4	88.42(6)	O7-Fe2-N8	176.44(6)
N1-Fe1-N2	84.20(9)	N5-Fe2-N6	80.85(11)	N1-Fe1-N2	91.60(6)	N5-Fe2-N6	78.96(6)
N1-Fe1-N3	161.85(9)	N5-Fe2-N7	168.41(10)	N1-Fe1-N3	175.30(6)	N5-Fe2-N7	162.71(6)
N1-Fe1-N4	91.34(9)	N5-Fe2-N8	91.89(11)	N1-Fe1-N4	91.74(6)	N5-Fe2-N8	91.36(6)
N2-Fe1-N3	78.30(10)	N6-Fe2-N7	88.04(10)	N2-Fe1-N3	85.09(6)	N6-Fe2-N7	84.56(6)
N2-Fe1-N4	83.88(9)	N6-Fe2-N8	87.38(10)	N2-Fe1-N4	90.20(6)	N6-Fe2-N8	83.65(6)
N3-Fe1-N4	91.56(9)	N7-Fe2-N8	90.88(11)	N3-Fe1-N4	91.60(6)	N7-Fe2-N8	92.00(6)

Table S3. Averaged bond angles (deg) in chromophores {FeN₄O₂} of complex **1**.

1a, unit A		1a, unit B		1b, unit A		1b, unit B	
O-Fe1-O	95.57	O-Fe2-O	93.64	O-Fe1-O	91.42	O-Fe2-O	95.42
N-Fe1-N	98.52	N-Fe2-N	101.24	N-Fe1-N	104.26	N-Fe2-N	98.87
O-Fe1-N	111.99	O-Fe2-N	111.86	O-Fe1-N	111.90	O-Fe2-N	111.93

Mononuclear Fe(III) Complex Showing Thermally Induced Spin Crossover and Slow Magnetic Relaxation with Reciprocating Thermal Behaviour

Terézia Bridová, Cyril Rajnák, Ján Titiš, Erika Samoľová, Kevin Tran, Ondrej Malina, Alina Bieňko, Franz Renz, Milan Gembický and Roman Boča

Table S4. Structural parameters for $[\text{Fe}^{\text{III}}(\text{L}^{\text{e/m}})\text{X}]$ complexes.

	Compound	T/K		Fe-N _{am}	Fe-N _{im}	Fe-X _{tail}	Fe-N _{av}	Fe-O _{av}	Σ /deg	Ref
1a	$[\text{Fe}(\text{L}^{\text{e}})(\text{NCSe})]$ A	293	SC	2.225	2.086	2.160	2.139	1.929	63.28	tw
	$[\text{Fe}(\text{L}^{\text{e}})(\text{NCSe})]$ B	293	HS	2.132	2.046	2.128	2.088	1.902	39.80	
1b	$[\text{Fe}(\text{L}^{\text{e}})(\text{NCSe})]$ A	100	SC	2.006	1.941	1.986	1.968	1.868	23.43	tw
	$[\text{Fe}(\text{L}^{\text{e}})(\text{NCSe})]$ B	100	HS	2.211	2.095	2.156	2.139	1.933	56.17	
2a	$[\text{Fe}(\text{L}^{\text{e}})(\text{NCS})]$ A	298	HS	2.194	2.081	2.080	2.118	1.928	50.5	[S8]
	$[\text{Fe}(\text{L}^{\text{e}})(\text{NCS})]$ B	298	HS	2.201	2.085	2.069	2.118	1.928	58.2	
2b	$[\text{Fe}(\text{L}^{\text{e}})(\text{NCS})]$ A	100		2.182	2.083	2.082	2.116	1.929	50.4	
	$[\text{Fe}(\text{L}^{\text{e}})(\text{NCS})]$ B	100		2.200	2.090	2.076	2.122	1.936	59.3	
2c	$[\text{Fe}(\text{L}^{\text{e}})(\text{NCS})]$ A	15	LS*	2.013	1.940	1.947	1.967	1.886	22.5	
	$[\text{Fe}(\text{L}^{\text{e}})(\text{NCS})]$ B	15	LS*	2.015	1.943	1.938	1.965	1.891	28.4	
3	$[\text{Fe}(\text{L}^{\text{e}})(\text{CN})]\cdot\text{H}_2\text{O}$	304	LS	2.010	1.944	1.975	1.976	1.904	20.8	[S9]
4	$[\text{Fe}(\text{L}^{\text{m}})(\text{NCO})]\cdot\text{MeOH}$	298	HS	2.218	2.078	2.081	2.126	1.946	54.0	[S9]
5	$[\text{Fe}(\text{L}^{\text{m}})(\text{N}_3)]$	298	HS	2.211	2.085	2.085	2.127	1.936	57.4	[S9]
6	$[\text{Fe}(\text{L}^{\text{m}})(\text{CN})]\cdot\text{MeOH}$	301	LS	2.028	1.935	1.971	1.978	1.904	26.0	[S9]

$\text{L}^{\text{e}} = 3\text{-EtO-salpet}$. $\text{L}^{\text{m}} = 3\text{-MeO-salpet}$. T = cell measurement temperature. $\text{X} = \text{NCSe}, \text{NCS}, \text{CN}, \text{NCO}, \text{N}_3$. Σ = Octahedral distortion angle is calculated from twelve *cis* angles within the chromophore $\{\text{FeN}_4\text{O}_2\}$. Fe-N_{im} = average of two bonds. [S8] P. Masárová, P. Zoufalý, J. Moncol, I. Nemeč, J. Pavlík, M. Gembický, Z. Trávníček, R. Boča and I. Šalitroš, *New J. Chem.*, 2015, **39**, 508. [S9] I. Nemeč, R. Herchel, R. Boča, Z. Trávníček, I. Svoboda, H. Fuessd and W. Linert, *Dalton Trans.*, 2011, **40**, 10090.

*the low temperature value of about 2.7 μB suggests the presence of a small amount of a remnant HS fraction.

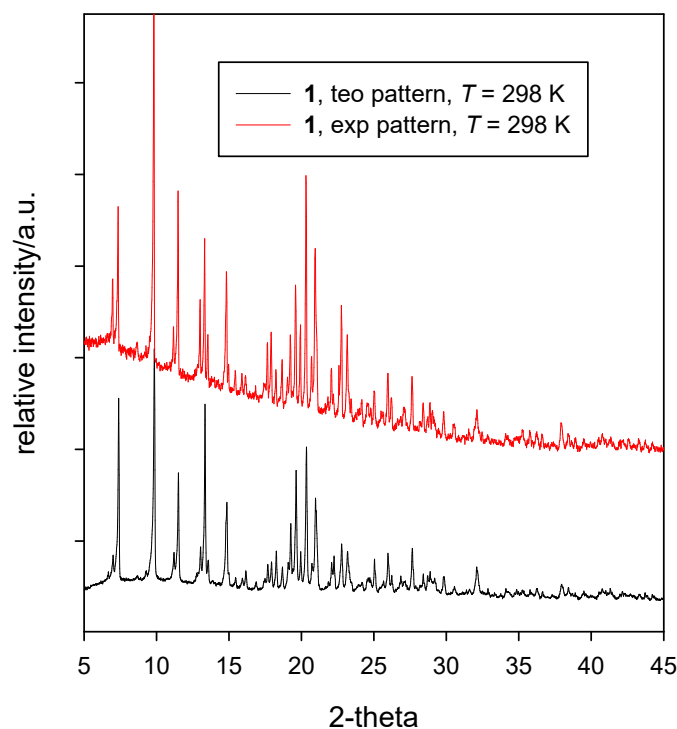


Figure S5. Calculated powder diffraction pattern for **1** from cif-file (teor), and recorded pattern at $\text{Cu } \lambda = 1.54060 \text{ \AA}$ (exp).

Mononuclear Fe(III) Complex Showing Thermally Induced Spin Crossover and Slow Magnetic Relaxation with Reciprocating Thermal Behaviour

Terézia Bridová, Cyril Rajnák, Ján Titiš, Erika Samoľová, Kevin Tran, Ondrej Malina, Alina Bieňko, Franz Renz, Milan Gembický and Roman Boča

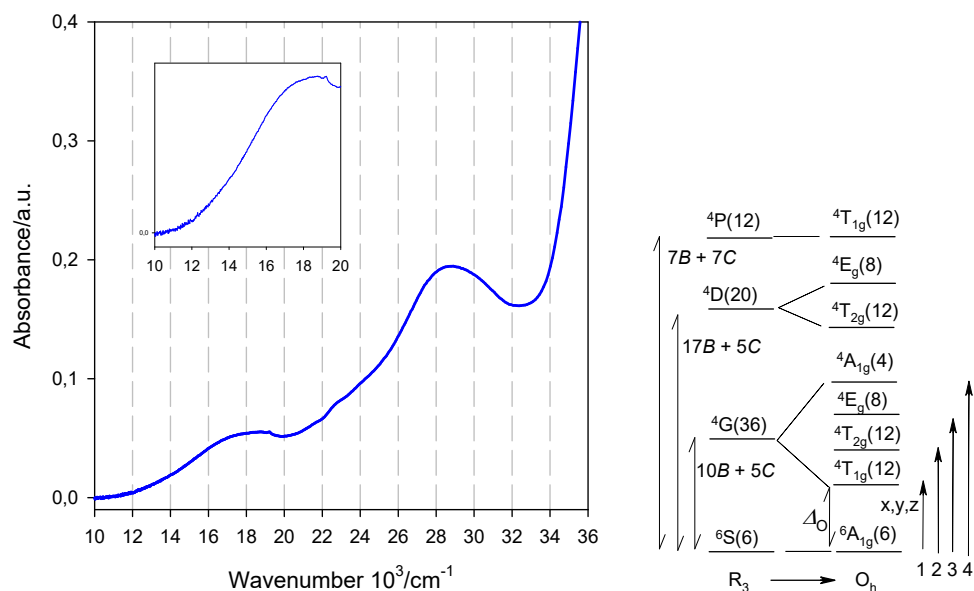


Figure S6. UV/Vis spectrum of **1** at room temperature and scheme of electronic terms. Visible d-d transitions are at 18000 [${}^6A_1 \rightarrow {}^4T_2(G)$], 24000 [${}^6A_1 \rightarrow {}^4A_1(G) + {}^4E(G)$], and 29000 [${}^6A_1 \rightarrow {}^4T_2(D) + {}^4E(D)$] cm^{-1} . The gerade index is dropped when the octahedral symmetry is disrupted. B and C are the Racah parameters of interelectron repulsion; Δ_O – octahedral crystal-field splitting parameter.

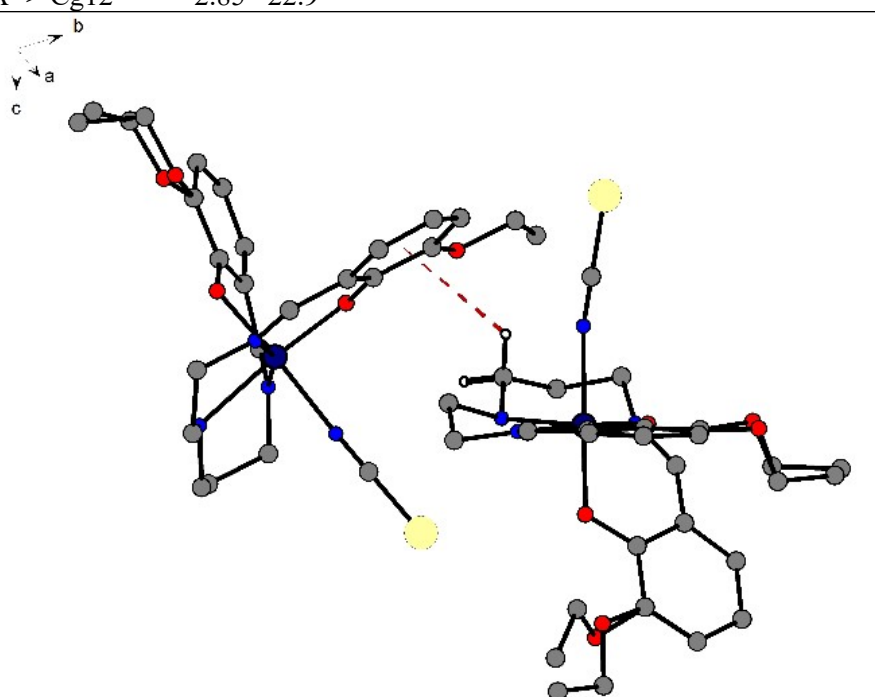
Table S5. Mössbauer spectra parameters for **1** at $T = 293$ K and $T = 77$ K.

	$\delta_{\text{IS}}/\text{mm}\cdot\text{s}^{-1}$	$\Delta E_Q/\text{mm}\cdot\text{s}^{-1}$	Site population/%
293 K			
Fe(III) HS	0.396 ± 0.010	0.882 ± 0.018	100
77 K			
Fe(III) HS	0.642 ± 0.044	1.244 ± 0.087	40.1 ± 4.2
Fe(III) LS	0.2233 ± 0.0031	2.8348 ± 0.0060	59.9 ± 1.8

Mononuclear Fe(III) Complex Showing Thermally Induced Spin Crossover and Slow Magnetic Relaxation with Reciprocating Thermal Behaviour

Terézia Bridová, Cyril Rajnák, Ján Titiš, Erika Samoľová, Kevin Tran, Ondrej Malina, Alina Bieňko, Franz Renz, Milan Gembický and Roman Boča

Table S6. Some intermolecular contacts.

1a, 293 K					
	D - H	H...A	D...A	D - H...A	
N2 ⁱ --H2 ⁱ ..Se2	0.98	2.81	3.716(3)	154	
N6 --H6 ..Se1	0.98	2.65	3.510(3)	147	
i: x, 1+y, z					
X--H(I)	Res(I)	Cg(J)	H..Cg	Gamma	
C34	-H34A	-> Cg12	2.85	22.9	
					
1b, 100 K					
	D - H	H...A	D...A	D - H...A	
N2 ⁱ --H2 ⁱ ..Se2	1.00	2.65	3.522(2)	146	
N6 --H6 ..Se1	1.00	2.69	3.628(2)	157	
i: x, -1+y, z					
X--H(I)	Res(I)	Cg(J)	H..Cg	Gamma	
C10	-H10B	-> Cg11	2.57	12.5	
C44	-H44B	-> Cg12	3.00	22.1	
C22A	-H22D	-> Cg5	2.85	14.3	

Mononuclear Fe(III) Complex Showing Thermally Induced Spin Crossover and Slow Magnetic Relaxation with Reciprocating Thermal Behaviour

Terézia Bridová, Cyril Rajnák, Ján Titiš, Erika Samoľová, Kevin Tran, Ondrej Malina, Alina Bieňko, Franz Renz, Milan Gembický and Roman Boča

AC susceptibility for the two-set Debye model

a) the in-phase component

$$\chi'(\omega) = \chi_S + (\chi_{T1} - \chi_S) \frac{1 + (\omega\tau_1)^{1-\alpha_1} \sin(\pi\alpha_1/2)}{1 + 2(\omega\tau_1)^{1-\alpha_1} \sin(\pi\alpha_1/2) + (\omega\tau_1)^{2-2\alpha_1}} \\ + (\chi_{T2} - \chi_{T1}) \frac{1 + (\omega\tau_2)^{1-\alpha_2} \sin(\pi\alpha_2/2)}{1 + 2(\omega\tau_2)^{1-\alpha_2} \sin(\pi\alpha_2/2) + (\omega\tau_2)^{2-2\alpha_2}}$$

b) the out-of-phase component

$$\chi''(\omega) = (\chi_{T1} - \chi_S) \frac{(\omega\tau_1)^{1-\alpha_1} \cos(\pi\alpha_1/2)}{1 + 2(\omega\tau_1)^{1-\alpha_1} \sin(\pi\alpha_1/2) + (\omega\tau_1)^{2-2\alpha_1}} \\ + (\chi_{T2} - \chi_{T1}) \frac{(\omega\tau_2)^{1-\alpha_2} \cos(\pi\alpha_2/2)}{1 + 2(\omega\tau_2)^{1-\alpha_2} \sin(\pi\alpha_2/2) + (\omega\tau_2)^{2-2\alpha_2}}$$

with the constraint for the isothermal susceptibilities $\chi_S < \chi_{T1} < \chi_{T2} = \chi_T$ in order to get positive contributions from each primitive component. The mole fractions fulfil

$$(\chi_{T1} - \chi_S) = (\chi_T - \chi_S)x_1, \quad (\chi_{T2} - \chi_{T1}) = (\chi_T - \chi_S)x_2, \\ x_1 = (\chi_{T1} - \chi_S)/(\chi_T - \chi_S), \quad x_2 = (\chi_{T2} - \chi_{T1})/(\chi_T - \chi_S), \quad \chi_{T2} = \chi_T, \quad x_2 = 1 - x_1.$$

The extension to the three-set Debye model is obvious.

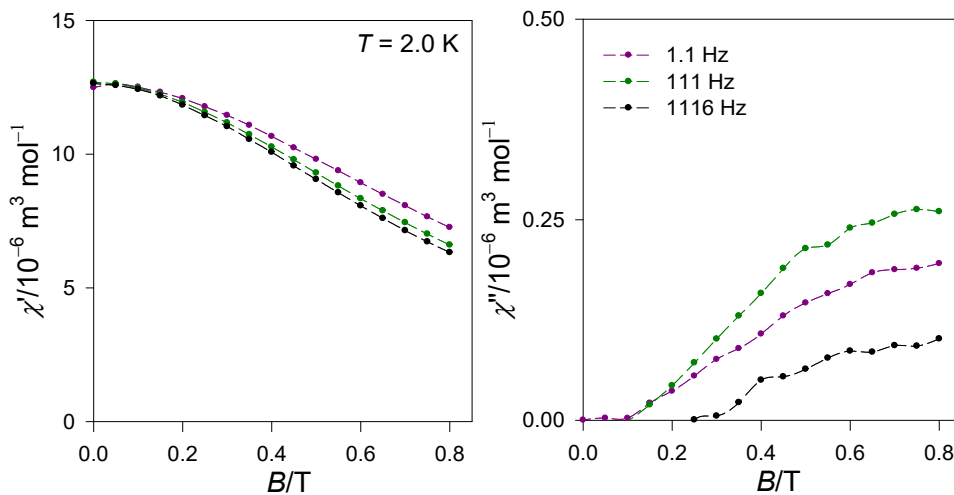


Figure S7. Field-frequency dependence of the AC susceptibility at $T = 2.0$ K for **1**.

Mononuclear Fe(III) Complex Showing Thermally Induced Spin Crossover and Slow Magnetic Relaxation with Reciprocating Thermal Behaviour

Terézia Bridová, Cyril Rajnák, Ján Titiš, Erika Samoľová, Kevin Tran, Ondrej Malina, Alina Bieňko, Franz Renz, Milan Gembický and Roman Boča

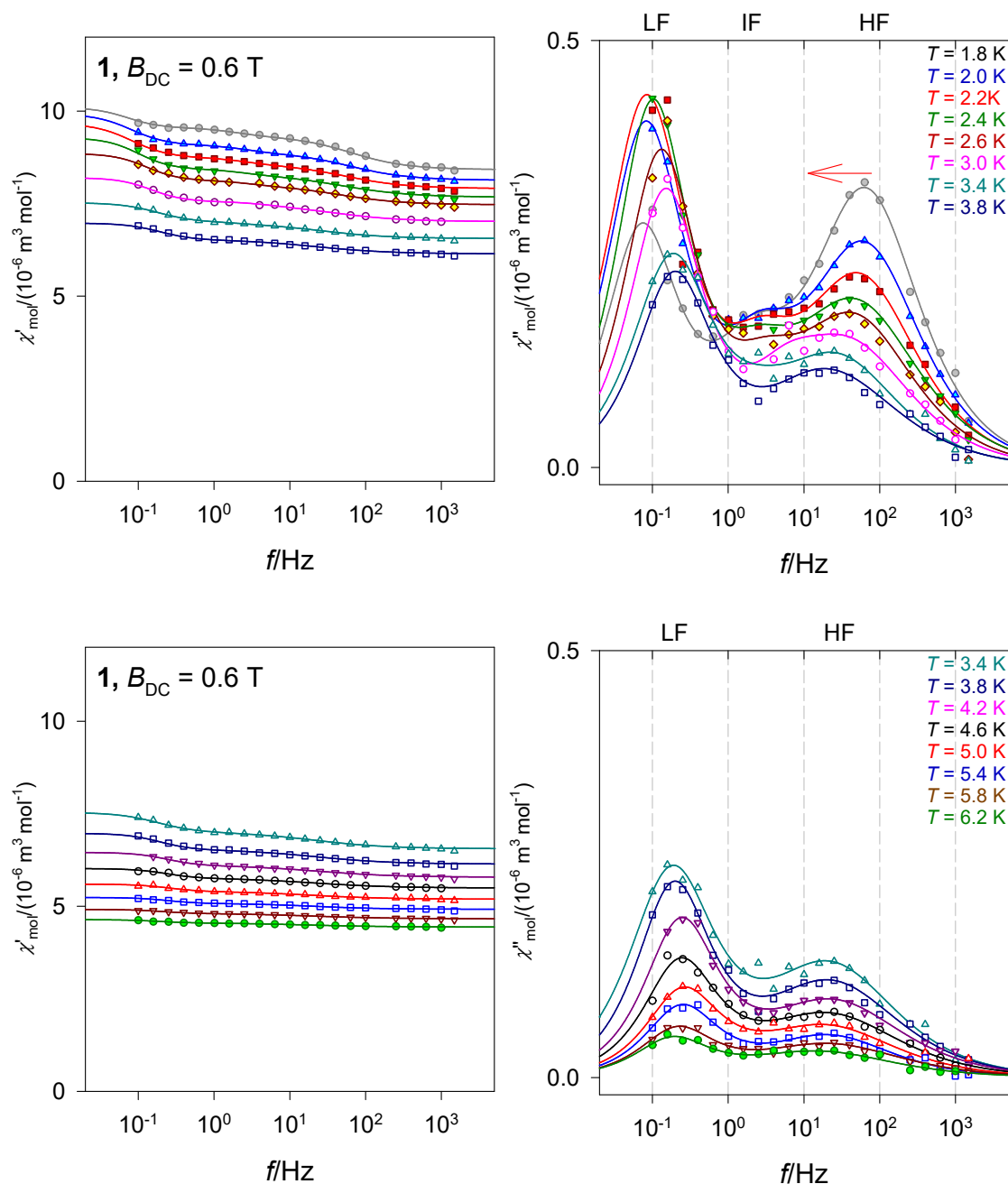


Figure S8. In-phase and out-of-phase AC susceptibility along with fitted lines. Top panel – three set Debye model, bottom – two set (intermediate frequency mode escaped). Red arrow envisages the reciprocating thermal behaviour.

Mononuclear Fe(III) Complex Showing Thermally Induced Spin Crossover and Slow Magnetic Relaxation with Reciprocating Thermal Behaviour

Terézia Bridová, Cyril Rajnák, Ján Titiš, Erika Samoľová, Kevin Tran, Ondrej Malina, Alina Bieňko, Franz Renz, Milan Gembický and Roman Boča

Table S7. AC susceptibility parameters for **1** at $B_{DC} = 0.6$ T using three-set and two set (for higher temperature) Debye model.

T/K	$R(\chi)$ /%	$R(\chi')$ /%	χ_S	χ_{LF}	α_{LF}	τ_{LF} /s	χ_{IF}	α_{IF}	τ_{IF} /s	χ_{HF}	α_{HF}	τ_{HF} / $10^{-3}s$	χ_{LF}	χ_{HF}
1.8	0.27	4.6	8.4(1)	9.0(3)	.0	2.2(8)	9.2(2)	.0(2)	80(23)	10(2)	.2(1)	2.5(3)	.32	.54
2.0	0.21	2.6	8.1(1)	8.9(1)	.0	2.0(3)	9.1(3)	.0(2)	60(12)	9.9(1)	.2(1)	2.5(3)	.47	.43
2.2	0.31	8.9	7.9(1)	8.8(2)	.1	1.9(5)	9.0(2)	.0(4)	60(24)	9.7(2)	.3(1)	2.9(9)	.53	.38
2.4	0.40	3.5	7.7(1)	8.5(2)	.0	1.6(3)	8.6(2)	.0(6)	64(40)	9.3(1)	.3(1)	3.3(17)	.52	.39
2.6	0.35	7.1	7.5(1)	8.2(1)	.0	1.2(1)	8.3(2)	.0(6)	52(32)	8.9(1)	.3(1)	3.4(18)	.52	.39
3.0	0.24	4.8	7.0(1)	7.6(1)	.0	1.08(7)	7.8(3)	.0(6)	29(20)	8.2(1)	.3(1)	3.7(41)	.54	.38
3.4	0.29	6.1	6.6(1)	7.1(1)	.0	0.89(12)	7.1(2)	.1	53	7.5(1)	.3(1)	5.0(46)	.53	.39
3.8	0.36	5.3	6.1(1)	6.6(2)	.0	0.83(10)	6.6(10)	.0	14	7.0(1)	.3(1)	5.5(21)	.54	.41
3.8	0.35	5.6	6.1(1)	6.6(1)	.0	0.83(7)				7.0(3)	.3(1)	7.0(14)	.53	.47
4.2	0.28	4.9	5.8(1)	6.1(1)	.0	0.67(7)				6.5(1)	.3(1)	6.6(14)	.52	.48
4.6	0.22	5.6	5.5(1)	5.7(1)	.0	0.68(5)				6.0(1)	.3(1)	7.5(14)	.49	.51
5.0	0.28	7.5	5.2(1)	5.4(1)	.0	0.63(7)				5.6(1)	.3(1)	8.1(23)	.47	.53
5.4	0.25	7.1	4.9(1)	5.1(1)	.0	0.65(7)				5.2(1)	.3(1)	7.3(17)	.50	.50
5.8	0.21	7.4	4.7(1)	4.8(1)	.0	0.75(10)				4.9(1)	.4(1)	7.5(21)	.42	.58
6.2	0.15	8.6	4.4(1)	4.5(1)	.0	0.87(12)				4.6(1)	.4(1)	9.9(29)	.42	.58
6.6	0.25	27	4.2(1)	4.3(1)	.0	1.00(32)				4.4(1)	.4(1)	10.7(77)	.41	.59

^a χ in units of $10^{-6} \text{ m}^3 \text{ mol}^{-1}$; $R(\chi)$ and $R(\chi')$ – discrepancy factors. Standard deviations in parentheses: 7.2(18) means 7.2 ± 1.8 ; 7.2(3) means 7.2 ± 0.3 .

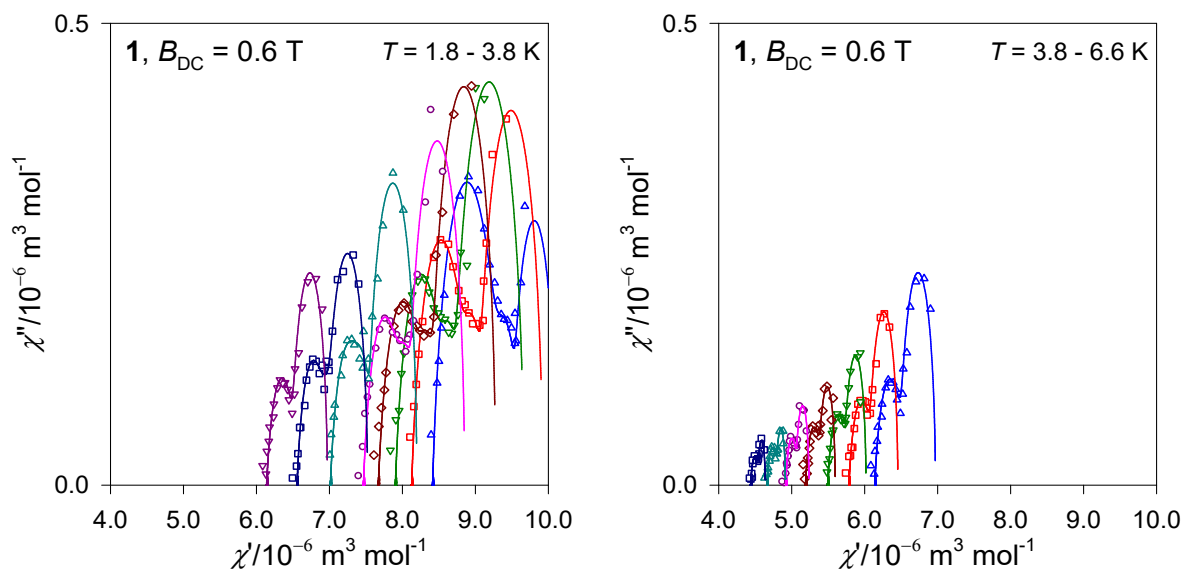


Figure S9. Argand diagram for **1** based on three-set (left) and two-set (right) Debye model.